

Magnetic Horn Optics: Exact Formulation vs. Paraxial Approximation for Low-Momentum (200 MeV/c) Capture

Comparison of Mathematical Models

Exact Formulation (Used for $p_z = 200$ MeV/c Optics)	Approximated Formulation (From Appendix of NuMI paper)
<p>1. Longitudinal Momentum (p_z):</p> $p_z(r) = p_{z,0} \pm \frac{q\mu_0 I}{2\pi} \ln\left(\frac{r}{r_{in}}\right) \quad (1)$	<p>1. Longitudinal Momentum (p_z): Assumed constant due to paraxial approx ($\ddot{z} \approx 0$).</p> $p_z(r) \approx p_{z,0} \quad (7)$
<p>2. Radial Momentum (p_r):</p> $p_r(r) = \sqrt{p^2 - [p_z(r)]^2} \quad (2)$	<p>2. Radial Equation of Motion:</p> $\frac{d^2 r}{dz^2} \approx -\frac{q\mu_0 I}{2\pi p_{z,0}} \frac{1}{r} \quad (8)$
<p>3. Trajectory Differential Equation:</p> $\frac{dr}{dz} = \frac{\sqrt{p^2 - [p_z(r)]^2}}{p_z(r)} \quad (3)$	<p>3. Trajectory Differential Equation: Approximated for small angles ($p_r/p_z \approx \theta$).</p> $\frac{dr}{dz} \approx \theta \quad (9)$
<p>4. Path Length in Field (Δz): Exact integration substituting $p_z = p \sin \phi$.</p> $\Delta z = \int_{\frac{\pi}{2}-\theta_0}^{\frac{\pi}{2}} \frac{r_{in} p}{K} \sin \phi \exp\left(\frac{p \sin \phi - p_{z,0}}{K}\right) d\phi \quad (4)$	<p>4. Path Length in Field (Δz): Approximated by the inner conductor's parabolic profile shape a.</p> $\Delta z \approx a \cdot r^2 \quad (10)$
<p>5. Deflection Angle (θ): Derived from exact momentum components at exit.</p> $\theta_{exit}(r) = \arctan\left(\frac{p_r(r)}{p_z(r)}\right) \quad (5)$	<p>5. Deflection Angle (θ): Simplified linear kick.</p> $\theta \approx \theta_0 - \frac{\mu_0 q I a}{2\pi p_{z,0}} r \quad (11)$
<p>6. Focal Length (f): Does not exist as a constant. Optics are highly non-linear.</p> $f_{eff}(r, \theta_0) = \frac{r}{\tan \theta_{exit} } \quad (6)$	<p>6. Focal Length (f): Assumes purely linear optics where f is a constant.</p> $f \approx \frac{2\pi p_{z,0}}{\mu_0 q I a} \quad (12)$ <p>(Resulting in $\theta \approx \theta_0 - \frac{r}{f}$)</p>

Why the Approximations Fail for $p_z = 200 \text{ MeV}/c$

The analytical model developed in the referenced technical paper brilliantly simplifies the horn optics by proving they act as predominantly linear focusing elements *for high-energy particles* ($p_z > 5 \text{ GeV}/c$). However, when optimizing for a $200 \text{ MeV}/c$ target, these approximations break down catastrophically due to the following physical realities:

1. **Failure of the Paraxial ($\ddot{z} \approx 0$) Assumption:** At $200 \text{ MeV}/c$, particles are emitted at very wide angles (e.g., 15°). To bend a 15° trajectory parallel to the axis, a massive amount of momentum must be transferred from the radial axis to the longitudinal axis by the Lorentz force. Treating $p_{z,0}$ as a constant denominator completely ignores this momentum transfer, mathematically violating the conservation of total momentum and artificially overestimating the focusing power of the horn.
2. **Failure of the Path Length Approximation ($\Delta z \approx ar^2$):** The paper assumes the path length inside the magnetic field is simply determined by the geometric parabolic profile of the conductor ($a \cdot r^2$). At large deflection angles, the particle's actual curved path is significantly longer than the geometric projection, requiring the exact trigonometric integral shown in Eq. 4.
3. **Failure of Linear Optics and Constant Focal Length (f):** The paper's angle formula ($\theta = \theta_0 - r/f$) defines a linear optical system with a fixed focal length f . At $200 \text{ MeV}/c$, the massive momentum transfers create extreme chromatic and spherical aberrations. A single focal length does not exist; f is highly dependent on the initial radius and angle, meaning the horn shape must be mapped perfectly to the exact non-linear equations rather than relying on a standard geometric parabola.

Simulated Output Geometries

The following plots map the continuous inner conductor surfaces for both the Forward (Horn 1) and Reverse (Horn 2) focusing elements, computed using the exact formulation defined above. Air/vacuum regions ($B = 0$) are explicitly modeled inside the thin aluminum shells.

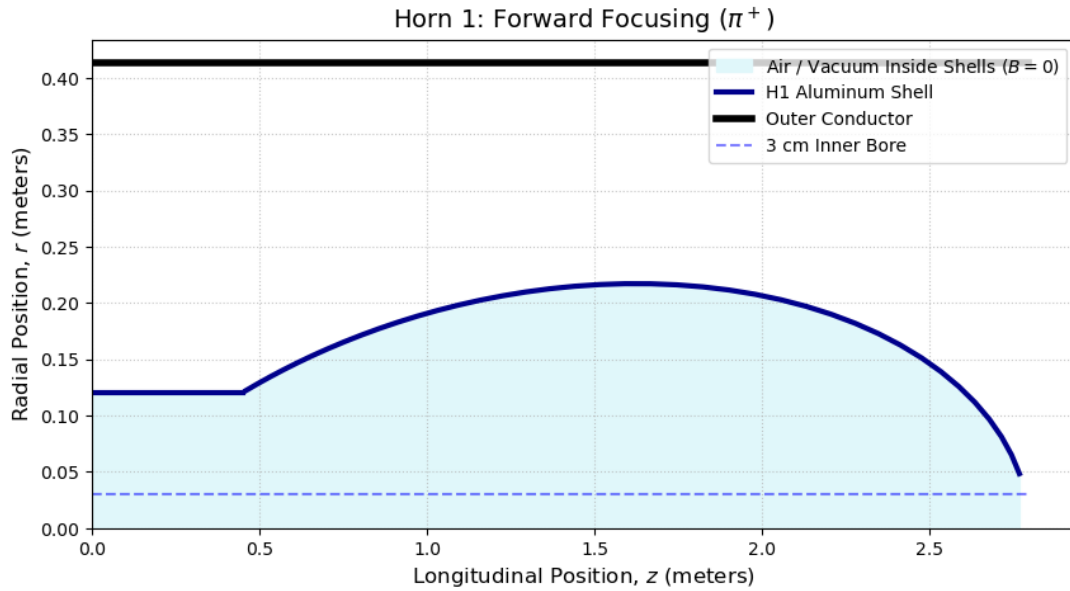


Figure 1: Optimized surface profile for Horn 1, capturing π^+ up to $\theta_{max} = 15^\circ$ at 100 kA. Particles emitted below 3° pass harmlessly through the 3 cm field-free bore.

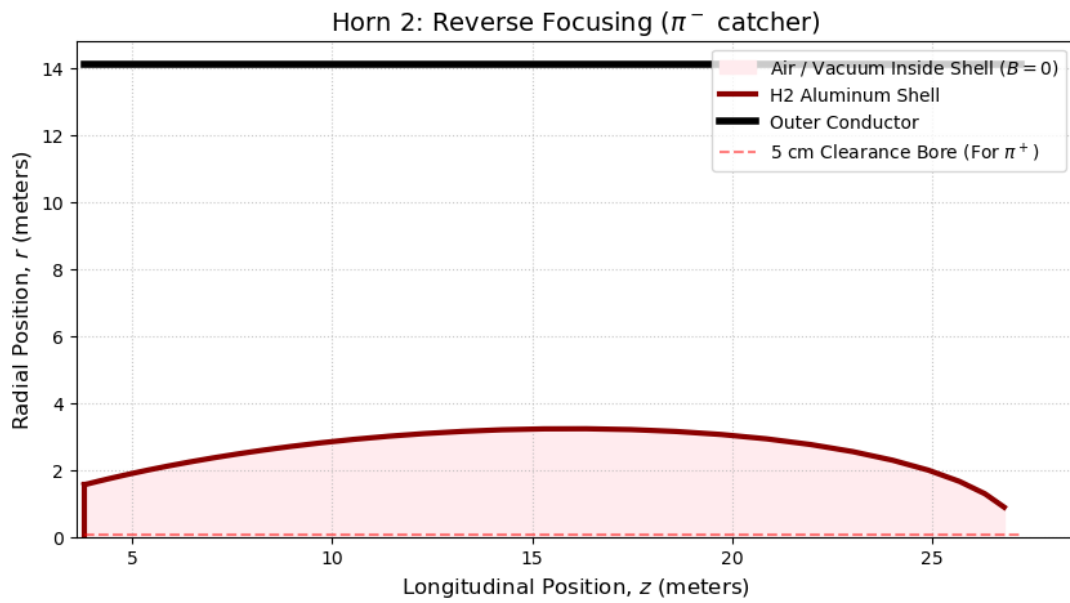


Figure 2: Optimized surface profile for Horn 2 (250 kA). Driven by the exact defocusing kinematics of Horn 1, this horn acts as a massive catcher for the widely dispersed π^- halo after a 1.0 m drift space, while maintaining a 5.0 cm clearance bore for the already-focused π^+ beam.